Streptococcal M Protein: Structural Studies of the Hypervariable Region, Free and Bound to Human C4BP†

I. André,‡ J. Persson,§ A. M. Blom,|| H. Nilsson,‡ T. Drakenberg,‡ G. Lindahl,§ and S. Linse*,‡

Department of Biophysical Chemistry, Lund University, Chemical Center, S-221 00 Lund, Sweden, Department of Laboratory Medicine, Division of Medical Microbiology, Lund University, Sölvegatan 23, S-223 62 Lund, Sweden, and Department of Laboratory Medicine, Division of Clinical Chemistry, Lund University, University Hospital Malmö, S-205 02 Malmö, Sweden

Received December 1, 2005; Revised Manuscript Received February 3, 2006

ABSTRACT: *Streptococcus pyogenes* is a Gram-positive bacterium that causes several diseases, including acute tonsillitis and toxic shock syndrome. The surface-localized M protein, which is the most extensively studied virulence factor of *S. pyogenes*, has an ∼50-residue *N*-terminal hypervariable region (HVR) that plays a key role in the escape of the host immunity. Despite the extensive sequence variability in this region, many HVRs specifically bind human C4b-binding protein (C4BP), a plasma protein that inhibits complement activation. Although the more conserved parts of M protein are known to have dimeric coiled-coil structure, it is unclear whether the HVR also is a coiled coil. Here, we use nuclear magnetic resonance (NMR) to study the conformational properties of HVRs from M4 and M22 proteins in isolation and in complex with the M protein binding portion of C4BP. We conclude that the HVRs of M4 and M22 are folded as coiled coils and that the folded nucleus of the M4 HVR has a length of ∼27 residues. Moreover, we demonstrate that the C4BP binding surface of M4-N is found within a region of four heptad repeats. Using molecular modeling, we propose a model for the structure of the M4 HVR that is consistent with our experimental information from NMR spectroscopy.

Streptococcus pyogenes (Group A Streptococcus) is a common human pathogen that causes a wide variety of diseases ranging from relatively mild throat and skin infections to life-threatening conditions such as the streptococcal toxic shock syndrome. The most extensively studied virulence factor of *S. pyogenes* is the surface-exposed M protein, which inhibits phagocytosis (*1*). This surface protein has an ∼50 residue *N*-terminal hypervariable region (HVR[1]), which varies extensively in sequence between different bacterial strains and allows the subdivision of clinical *S. pyogenes* isolates into >100 different M types (*2*). Importantly, protective antibodies are directed against the HVR, but because of the sequence variability, the immunity is type-specific. Thus, the HVR gives rise to the so-called antigenic variation in M proteins.

Despite the extensive sequence variability between HVRs, many M proteins specifically bind the human plasma protein C4b-binding protein (C4BP) (*3*−*7*), an inhibitor of classical pathway complement activation (*8*−*10*). When bound to streptococci, C4BP retains its complement regulatory function and contributes to the ability of the bacteria to resist phagocytosis because bound C4BP decreases complement deposition on the bacterial surface (*3*, *11*). Studies of C4BP-binding HVRs have been much facilitated by the finding that they can be studied as synthetic peptides, dimerized via a *C*-terminal cysteine, which retain the ability to specifically bind C4BP (*6*). Thus, the structural and immunological properties of different HVRs can be directly compared. Interestingly, the isolated C4BP-binding HVRs studied so far, completely lack immunological cross-reactivity (*6*), although they specifically bind the same ligand and might be expected to have similar structures. One possible explanation for this apparent paradox is that C4BP and antibodies employ separate modes of binding to the HVR.

There is strong evidence that M proteins adopt a dimeric coiled-coil structure (*12*−*15*), but it is unclear whether the coiled coil extends through the HVR. This is an important problem because the HVR may be of key importance in the ability of M protein to promote virulence and because efforts are under way to develop an *S. pyogenes* vaccine on the basis of a combination of HVRs (*16*). Analysis of the structure of different HVRs is also of considerable interest with regard to protein folding because HVRs with very few residue identities specifically bind the same ligand, human C4BP.

Here, we have studied the conformational properties of HVRs from the M4 and M22 proteins (peptides M4-N and M22-N and the longer M22-NL, see Figure 1) in isolation and in complex with an M protein-binding fragment of C4BP (C4BPα-CCP1-2) using nuclear magnetic resonance (NMR).

† This study was supported by Swedish Research Council grants to A.B., T.D., G.L., and S.L.

* Corresponding author. Tel: +46-46-222-8246. Fax: +46-46-222-4543. E-mail: sara.linse@bpc.lu.se.

‡ Department of Biophysical Chemistry.

§ Division of Medical Micobiology.

|| Division of Clinical Chemistry.

[1] Abbreviations: C4BP, C4b-binding protein; HSQC, heteteronuclear single quantum coherence; HVR, hypervariable region; M22-N, residues 1−52 of M22 with an added *C*-terminal cysteine; M22-NL, residues 1−83 of M22 with an added *C*-terminal cysteine; M4-N, residues 1−45 of M4 with an added *C*-terminal cysteine; NMR, nuclear magnetic resonance; NOE, nuclear Overhauser effect; NOESY, nuclear Overhauser effect spectroscopy; PFG, pulse field gradient; RDC, residual dipolar couplings; TOCSY, total correlation spectroscopy; TROSY, transversed relaxation optimized spectroscopy.

10.1021/bi052455c CCC: $33.50
Published on Web 03/17/2006

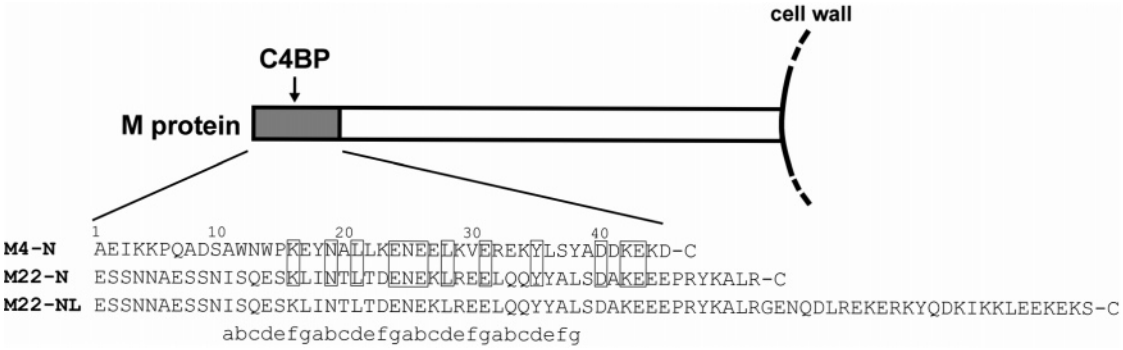

FIGURE 1: Sequences of peptides used in this study and their positions within the full-length streptococcal M protein on the bacterial surface. Note that all peptides include a *C*-terminal cysteine residue, which is not present in the intact M protein. Identities between the M4-N and M22-N sequences are boxed, and the heptadic repeat pattern, as predicted by COILS (*31*), is indicated in the region predicted to interact with C4BP.

Because of the hydrodynamic properties of the molecules, molecular exchange and aggregation, structure determination of the peptides was not possible. However, using a variety of techniques, we obtained clear indications that M4-N is folded and largely adopts a coiled-coil structure in solution. We could also identify the parts of M4-N that are folded, and we could map the binding surface in M4-N for C4BPα-CCP1-2. Interestingly, our data further suggest that M4-N and M22-N adopt similar folds, both in solution and in complex with C4BPα-CCP1-2, despite the extensive difference in primary sequence between these two C4BP-binding domains.

MATERIALS AND METHODS

Expression and Purification of Peptides Derived from M Proteins. The 5′ end of the genes encoding the M4 and M22 proteins were amplified from plasmids pARP401 (*17*) and pSir2202 (*18*) and cloned into the pET3a expression vector. A *C*-terminal cystein was inserted into all constructs for dimerization purposes. The cloning was performed using standard PCR and DNA purification techniques. The genes were expressed in *Escherichia coli* (either ER2566 or BL21* cells) and grown in LB media (for unlabeled proteins), M9 media supplemented with a vitamin solution (1 mM $MgSO_4$, 0.1 mM $CaCl_2$, 18 μM $FeCl_2$, 1 μg/mL of vitamin B3) 0.64 g/L of $^{15}NH_4Cl$, and 3 g/L of glucose (for ^{15}N labeled protein), or M9 media supplemented with a vitamin solution, 1 g/L of $^{15}NH_4Cl$, and 1.5 g/L of ^{13}C glucose (for $^{15}N^{13}C$ labeled protein). The cells were induced with IPTG at OD values of 0.5−0.7 and harvested by centrifugation (5500*g* for 10 min) 4−5 h after induction.

Purification was achieved using ion exchange chromatography and gel filtration with typical sizes and volumes of columns and gradients as follows for a 4.5 liter culture. The cells were broken by osmotic shock or sonication. For M22-NL, the cells were resuspended in ∼160 mL of deionized and filtered H_2O (ddH_2O), heated to 80 °C after mixing with a boiling buffer (20 mM Tris-HCl at pH 7.5), then directly chilled on ice, and centrifuged at 13 000 rpm for 15 min. For M4-N and M22-N, the cell pellet was resuspended in ∼50 mL of 10 mM Tris-HCl at pH 7.5 and 1 mM EDTA, sonicated, and centrifuged at 13 000 rpm for 15 min. For all three proteins, the supernatant was then oxidized either by bubbling with air or by the addition of 20 μM $CuCl_2$ and incubation at pH 8.0 in 0.4 M NaCl for 5 h. The oxidized solution was then diluted 1:4 and applied onto a 3.4 × 18 cm DEAE-cellulose column and the sample eluted using a linear gradient between 0 and 400 mM NaCl in 20 mM Tris-HCl at pH 7.5. Appropriate fractions were collected, pooled, freeze-dried, and dissolved in 10 mL of water and applied to a G50 gel filtration column (3.4 × 200 cm) with 50 mM NaAc at pH 6.5 as the running buffer. Fractions containing protein were dialyzed against ddH_2O for 3 days with changes 3 times a day. The purity of the protein was analyzed by SDS−PAGE and ^1H NMR. Typical yields were, 20 mg/L, 30 mg/L, and 30 mg/L for M4-N, M22-N, and M22-NL, respectively. All concentrations reported are for the dimer form of the peptides.

Purification of C4BPα-CCP1-2. C4BPα-CCP1-2 was recombinantly expressed in *E. coli* and purified from inclusion bodies. DNA coding for C4BPα-CCP1-2 was amplified from cDNA coding for CCP1-2 of the C4BPα chain using PCR and the following primers, forward: 5′ TAT **CAT ATG** AAT TGT GGT CCT CCA CCC ACT TTA and reverse: 5′ TTG **GAG CTC** TTA AAG TGT AAC ACC CTC TCC TAG, with restriction sites marked in bold. The sequence of the resulting protein is **M**NCGPPPTLSFAAPMDITLTETRFKTGTTLKYTCLPGYVRSHSTQTLTCNSDGEWVYNTFCIYKRCRHPGELRNGQVEIKTDLSFGSQIEFSCSEGFFLIGSTTSRCEVQDRGVGWSHPLPQCEI**LEHHHHHH**, where extra amino acids not present in the original sequence are indicated in bold. The resulting product was cloned in a bluescript vector using a PCR-Script cloning kit (Stratagene), sequenced, and transferred into a pET26 vector (Novagen) using NdeI and XhoI restriction enzymes (Fermentas). The protein was expressed in BL21-CodonPlus RP bacteria (Stratagene). The cells were induced with IPTG at OD values of 0.6−0.8 and a reduction of temperature from 37 to 30 °C and harvested by centrifugation (5000*g* for 20 min). The pellet was resuspended in 200 mL of cold PBS buffer, centrifuged, and dissolved in 100 mL of cold PBS. Lysozyme (80 mg) was added, and the solution was incubated for 15 min at room temperature. The solution was sonicated on ice for 30 min and centrifuged (15 min at 5000*g*), and the cell pellet was washed twice with ice cold PBS. The inclusion bodies were resuspended in 6 M Guanidium-HCl, 20 mM Tris-HCl at pH 8.0, and 10 mM reduced glutathione and sonicated for 10 min to dissolve the pellet. The sonicate was then filtered through a 0.45 μm filter. The protein sample was applied to a Ni-NTA Superflow

column (~100 mL) (Qiagen), equilibrated with the same buffer that was used to dissolve the inclusion bodies, and then washed with 300 mL buffer. The protein was eluted with 6 M guanidium-HCl, 20 mM Tris-HCl at pH 8.0, 10 mM reduced glutathione, and 0.7 M imidazole. The eluted protein was refolded as previously described (*19*) by diluting the protein to 0.8 mg/mL in a refolding buffer (55 mM Tris-HCl at pH 8.5, 10.56 mM NaCl, 2.2 mM $CaCl_2$, 2.2 mM $MgCl_2$, 0.055% PEG4000, 0.55 M arginine, 0.1 mM oxidized glutathione, and 1 mM reduced glutathione) and incubated overnight with gentle stirring. Iodoacetamide (5 mM) was added to the refolding buffer, and the solution was incubated at 4 °C for 30 min. The solution was dialyzed against 50 mM Tris-HCl, at pH 8.5 and applied to a SourceQ column (~10 mL) (Amersham Biosciences) and equilibrated with a dialysis buffer, and the protein was eluted at 5 mL/min with a 50 mM Na-phosphate buffer at pH 8.5. The refolding reaction was monitored by studying the binding of a conformation-dependent monoclonal antibody-recognizing CCP1 of C4BPα chain to the protein (*20*).

Mass Spectrometry. Matrix absorption laser-assisted desorption/ionization mass spectrometry was performed by Swegene (Lund University, Sweden).

CD Spectroscopy. CD spectra (180−250 nm, response time 16 s, resolution 1 nm, scan rate 20 nm/min, 4 scans averaged) were obtained at 25 °C using a Jasco J-720 spectropolarimeter with a Jasco PTC-343 Peltier type thermostatic cell holder and a quartz cuvette with path lengths of 1 mm. The peptide concentration was 27−70 μM in 5 mM Tris-HCl at pH 7.5 or 0.03−0.75 mM for the aggregation study of M4-N. Temperature scans (15−80 °C at 1 °C/min) were monitored at 221 nm (bandwidth of 2 nm) and was conducted with concentrations in the range of 27−70 μM, and the data were analyzed using a two-state folding model to extract the temperature at the transition midpoint T_m by nonlinear least-squares fitting using the following equation

$$y = \frac{a_N + b_N T + (a_U + b_U T)\exp[-(\Delta H_{NU}(1 - T/T_m) - \Delta C_p(T_m - T - T\ln(T/T_m))]}{1 + \exp[-(\Delta H_{NU}(1 - T/T_m) - \Delta C_p(T_m - T - T\ln(T/T_m))]} \quad (1)$$

where a_N, b_N, a_U, and b_U are the intercepts and slopes of the baseline of the native and unfolded states, ΔH_{NU} is the enthalpy difference, ΔC_p the heat capacity difference between the folded and unfolded states, and T is the temperature. T_m is not significantly affected by the value of ΔC_p, which is not well specified by the fit.

Multidimensional Nuclear Magnetic Resonance Measurements. Unless otherwise indicated, the NMR data was acquired on a 600 MHz Varian UNITY PLUS spectrometer. The processing of NMR data was performed using NMRPipe (*21*) program suite, and Sparky (T. Goddard and T. Kneller, University of California at San Fransisco, unpublished results) was used for assignment and peak analysis. All data were acquired at 25 °C unless otherwise stated.

Sample Preparation for NMR. NMR samples contained 0.1 mM or 1 mM M4-N, M22-N, or M22-NL in H_2O with 10% D_2O, 0.2 mM NaN_3, and 0.1 mM DSS at pH 5.8−7.0 in a total volume of 300 μL in susceptibility matched NMR tubes (Shigemi, Tokyo, Japan). Complexes between M4-N, M22-N, M22-NL, and C4BPα-CCP1-2 were prepared using a 1:5 ratio between M protein and C4BPα-CCP1-2. C4BPα-CCP1-2 was concentrated using a spin concentrator (Vivaspin) with a MW cutoff of 5. The freeze-dried M protein was dissolved in this solution, and the pH was adjusted to 7.5.

Backbone Assignment. 2D ^{15}N-^{1}H HSQC (*22*), HNCA (*23*), and CACB(CO)NH (*24*) spectra were collected to determine the chemical shifts of ^{1}H, ^{15}N of amide groups and ^{13}C resonances of α and β carbons. For the acquisition of HNCA and CBCA(CO)NH, 32 points were collected in ω1 with 50 and 1024 points in ω2 and ω3, respectively. For HNCA and CBCA(CO)NH, 16 and 32 transients, respectively, were collected. HNCO spectra were collected on a Varian Unity 500 MHz spectrometer, with 8 transients and with 40, 96, and 1024 points collected in ω1, ω2, and ω3, respectively. A HCACOCANH spectrum was also collected to provide sequential assignments based on backbone carbonyl chemical shifts (*25*). HCACOCANH provides correlations between HN(i), N(i), CO(i-1), and CO(i) and was collected with 40, 32, and 1024 points in ω1, ω2, and ω3, respectively. Thirty-two transients were acquired for this experiment. The spectra were processed in NMRPipe with linear predictions in the indirect domain and zero-filling to give data sets with dimensions of 512 × 512 × 1024 points in ω1, ω2, and ω3. TOCSY, NOESY, and HSQC-TOCSY spectra were acquired with standard parameters.

Side-Chain Assignment. The CBCA(CO)NH pulse sequence was modified to correlate Asn, Gln $H^{\delta 2}$, or $H^{\epsilon 2}$ with C^{α} and C^{β} or C^{β} and C^{γ} by the optimization of the polarization delay for an NH_2-group and the carrier frequencies.

NMR Relaxation Measurements. Spin−lattice (R_1) and spin−spin (R_2) relaxation rate constants as well as {^{1}H}-^{15}N steady-state heteronuclear Overhauser enhancements (NOE) were measured using 2D pulsed field-gradient-enhanced experiments as described (*26*) using a 600 MHz Varian UNITY PLUS spectrometer operating at a ^{1}H frequency of 599.89 MHz. Spectra were acquired with 2048 complex points and a spectral width of 7500 Hz ω2 (^{1}H) and 128 complex points with a spectral width of 1800 Hz in ω1 (^{15}N). The recovery time between experiments was 1.5, 2.0, and 10.0 s for R_1, R_2, and {^{1}H}-^{15}N, respectively. The R_1 values were determined at 25 °C with the following relaxation delays: 2 (*2), 170, 320, 470 (*2), 620, 770 (*2), 920, 1220, 1370 (*2), and 1520 ms. The R_2 values were determined a 25 °C with the following relaxation delays: 2 (*2), 4, 6 (*2), 8 (*2), 10, 120, 140, 180, 250, and 300 (*2) ms, with (*2) indicating experimental duplicates. In the NOE experiment, two spectra were recorded interleaved, one with NOE and one without. All spectra were processed using the NMRPipe program suite with a Lorentzian-to-Gaussian transformation in ω2 and a shifted sinebell in ω1. The relaxation rates were estimated by the nonlinear least-squares fitting of an exponential function to the experimental data. Theoretical R_1 and R_2 values were calculated from a hydrodynamic simulation of the model structure of M4-N using the computer program HydroNMR (*27*).

Dipolar Couplings. Dipolar couplings of M4-N were measured in a 3% C12E5/*n*-hexanol medium (*28*) with a protein concentration of 0.1 mM in H_2O with 10% D_2O, 0.2 mM NaN_3, and 0.1 mM DSS at pH 6.0−7.0. $^{1}J_{NH}$ couplings for free and aligned samples were obtained from 2D ^{15}N-^{1}H IPAP HSQC spectra (*29*). The theoretical estimates of the

dipolar coupling were calculated from the model of M4-N using the computer program PALES (*30*).

Molecular Modeling. The heptadic repeat pattern of M4-N was predicted using COILS (*31*). The structure of M4-N was modeled onto the structure of the *C*-terminal SIR4 protein from *S. cerevisiae* (*32*) (pdb 1PL5) using the computer program Modeler 6.2 (*33*). The heptadic repeat sequence of M4-N was aligned to the heptadic repeats of SIR4.

RESULTS

Experimental System. Recombinant peptides derived from the M4 and M22 proteins were cloned and expressed in *E. coli*, and the design of the constructs is shown in Figure 1. Two different constructs derived from M22 were produced. The shorter one (M22-N, residues 1−52) includes the HVR with the binding site for C4BP (*6*). The longer construct (M22-NL, residues 1−83) extends into an adjacent semi-variable region, thereby including binding regions for both C4BP and IgA-Fc (*34*). The construct derived from the M4 protein (M4-N, residues 1−45) includes the HVR with the C4BP binding site. Because HVR peptides need to be dimeric to bind C4BP (*6*), all constructs were prepared with a *C*-terminal cysteine residue to facilitate dimerization through disulfide linkage. Microtiter-plate assays confirmed that all peptides could bind C4BP (data not shown). For M22-NL, which also contains an IgA binding site, the binding to IgA was established (data not shown). The molecular mass of dimerized M4-N was determined to be 11032 Da by MALDI mass spectrometry. This is 16 Da higher than expected and is probably a consequence of oxidation. The molecular mass obtained for M4-N indicates that the peptides that were expressed in *E. coli* do not have an *N*-terminal methionine.

Conformation and Stability of Peptides Studied by CD. The CD spectra of M4-N, M22-N, and M22-NL indicate that the peptides are folded in helical structures (Figure 2A). Coiled-coil proteins have been shown to have two minima at 208 and 221 nm, as observed for all three M-protein derived peptides. The ratio between the signal at 208 and 221 nm has been used as an indication of coiled-coil structure (*35*, *36*). Although our data are consistent with the peptides being folded as coiled coils, this ratio is probably not very useful for proteins with significant fractions of their residues in unstructured regions.

The stability toward thermal denaturation of the peptides was determined at pH 7.5 by following the CD signal arising from the peptide backbone at 221 nm (Figure 2B). The T_m values were determined by a least-squares-fitting of the data using a two-state model including one folded and one unfolded species (eq 1, Materials and Methods) yielding 39, 28, and 37 °C for M4-N, M22-N, and M22-NL, respectively. For M4-N, the two-state assumption is justified by the fact that identical T_m values were obtained when the unfolding equilibrium was followed at 208 and 221 nm. This shows that the helix (monitored at 221 nm) disappears as the coiled coil (monitored as the ratio between 208 and 221 nm) dissociates. M22-N has a less cooperative unfolding than the longer M22-NL, observed as an unfolding process that extends over a larger temperature range. M22-N is less stable than M22-NL, and the T_m value is not as well defined as that for the other two peptides. The T_m value for the M22-NL peptide is identical to the value for the intact M22 protein (37 °C) (*37*).

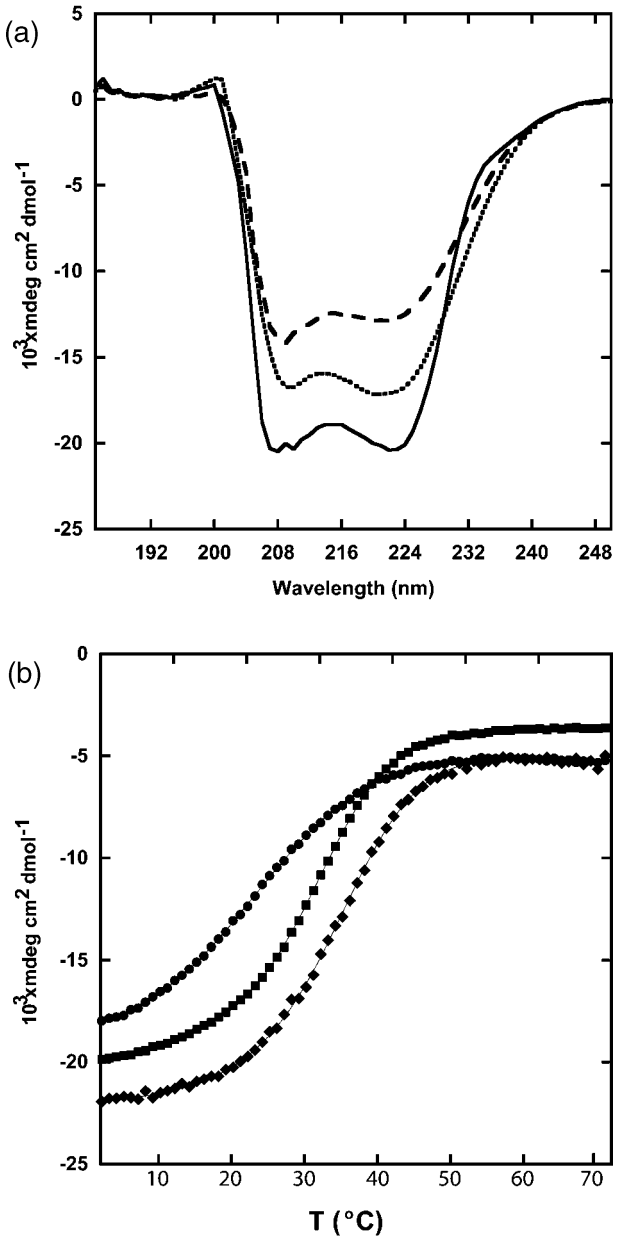

FIGURE 2: (A) CD spectra of M4-N (—), M22-N (---), and M22-NL (....) at 25 °C in 5 mM Tris-HCl at pH 7.5. (B) Temperature denaturation of M4-N (◆), M22-N (●), and M22-NL (■) in 5 mM Tris-HCl at pH 7.5, monitored by CD at 221 nm. The solid lines represent the computer fits of eq 1 to data.

Assignment of M4-N. Using triple resonance experiments, the M4-N ^{1}H-^{15}N HSQC spectrum was assigned at 1 mM protein concentration using standard procedures. Almost all residues (1−14 and 19−46) could be assigned despite the extensive signal overlap, the presence of extra peaks in the spectra, and the severe line broadening (Figure 3A). On the basis of these assignments, the molecular conformation as well as the C4BP-binding properties of M4-N and other peptides could be assessed, as outlined below.

Spectral Properties of Peptides. The ^{1}H-^{15}N HSQC spectra of M4-N, M22-N, and M22-NL display similar features (Figure 3). A folded globular protein typically has one peak for the backbone NH group of each residue (minus prolines and the *N*-terminal residue) and two peaks for each side-chain amide, and all NH peaks typically have similar line widths. This is not the case for the M peptides. For all three

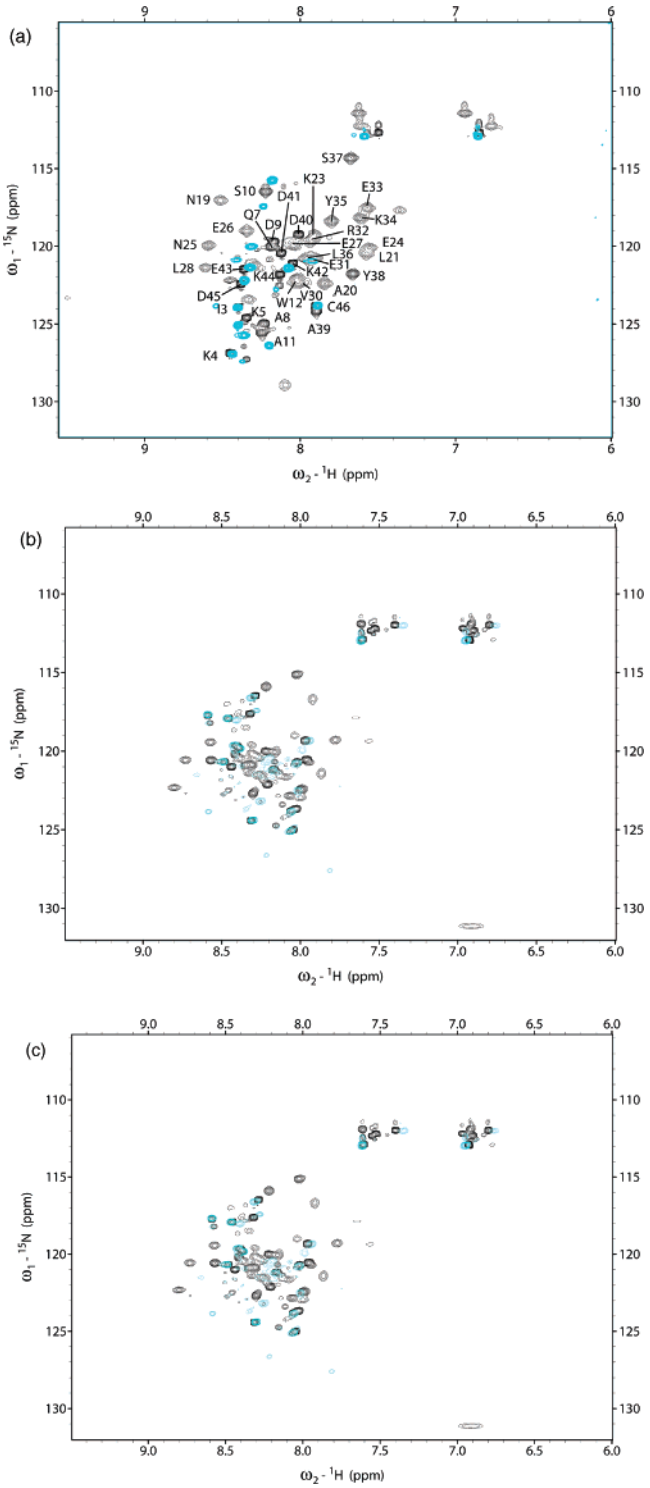

FIGURE 3: ^{1}H-^{15}N HSQC spectra of free peptides and peptides in complex with CCPα1-2 of C4BP. (A) M4-N free (black) and in complex with CCPα1-2 (cyan). The resonance assignments for free M4-N are indicated. (B) M22-N free (black) and in complex with CCPα1-2 (red). (C) M22-NL free (black) and in complex with CCPα1−2 (red).

peptides, a large number of sharp peaks were found, consistent with flexible residues, and the rest of the peaks were very broad. The broad peaks could be caused by a number of factors, as outlined below. The spectra did not allow a high-resolution structure determination by NMR because few NOESY cross-peaks were found, yielding a limited set of distance restraints. M4-N was chosen for more detailed studies because its ^{1}H-^{15}N HSQC spectrum displayed the least spectral overlap and the smallest number of broad cross-peaks.

A first possible cause of the line broadening found in M4-N is aggregation. The CD spectra of M4-N were therefore recorded as a function of protein concentration, and for the dimerized peptide, we found a large concentration dependence of the CD signal above 0.1 mM concentration. However, using PFG ^{1}H NMR, a method that can be used to study the mobility of protein molecules in solution, it was seen that the translational diffusion rate was independent of protein concentration in the range 0.1−1 mM, and in gel filtration, only one M4-N species was found. A comparison of the ^{1}H-^{15}N HSQC spectra of M4-N at 0.1 and 1 mM showed that some of the resonances move as a function of concentration. These changes were confined to the *N*-terminal part of the molecule, which is largely flexible in solution (see the section on dynamical properties of M4-N). The line broadening is reduced at low concentration. Mass spectra showed, in addition to the dimer, a mass that was twice that of the dimer, whereas gel filtration showed a maximum 0.7% tetramer, which is lost upon reduction with DTT, in parallel to the loss of dimers. Taken together, these data indicate that a loosely associated tetramer (dimer of dimers) is present in solution and that it associates via the flexible *N*-terminal parts.

A second factor that can cause line broadening is the extended shape of the peptides. In a coiled coil, all NH bond vectors point in the same direction, that is, the long axis of the molecule, and this could lead to extensive relaxation of magnetization. However, this is not likely to be the main cause of the observed line broadening because TROSY experiments, where line broadening caused by slow tumbling of proteins can be reduced, did not yield any significant spectral improvement. These experiments were conducted at 600 MHz for M4-N and at 800 MHz for M22-N and M22-NL at different temperatures.

A third cause of extensive line broadening could be the chemical exchange on a time scale of ∼0.1−100 ms. To evaluate this possibility, we recorded CPMG ^{1}H-^{15}N HSQC spectra using a pulse sequence designated for the removal of line broadening caused by chemical exchange. The CPMG ^{1}H-^{15}N HSQC spectrum of M4-N was clearly different from its regular ^{1}H-^{15}N HSQC spectrum, indicating chemical-exchange broadening. There were also a number of low intensity peaks in the M4-N spectrum in addition to the 43 peaks expected for the nonproline residues. This could be due to slow exchange processes (aggregation reactions or other types of exchange processes) or molecular heterogeneity. In the HCACOCANH spectra, multiple resonances were found for A8, D9, and A11, indicating a slow exchange process. This can be due to a cis−trans isomerization of P6. Also, N13−N19 could not be assigned because of missing resonances, and this may be due to the exchange processes associated with P15 isomerization. In the *C*-terminal part of the molecule, multiple resonances were seen for A39 and D40, again indicating that exchange processes are occurring at that site.

Comparison of ^{1}H-^{15}N Spectra of Peptides. M4-N, M22-N, and M22-NL (Figure 3) have 17, 27, and 17 very sharp peaks, respectively, consistent with flexible residues, leaving roughly 27, 25, and 65 residues, respectively, in an ordered

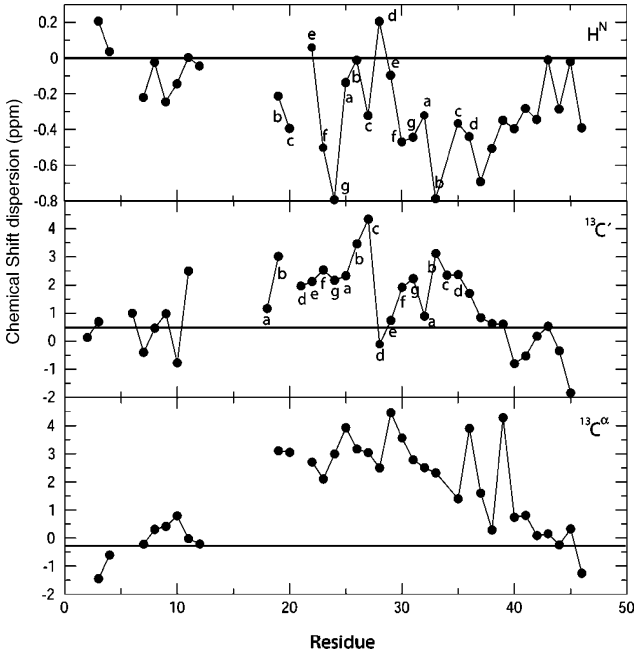

FIGURE 4: Displacement of the chemical shift of M4-N relative to the corresponding random coil values of Wütrich (*41*) ($^1H^N$) and Wishart and Sykes (*39*) ($^{13}C\alpha$ and $^{13}C'$). The heptadic repeat pattern as predicted by COILS is indicated. The horizontal lines indicate chemical-shift displacements consistent with an α-helical conformation (*38*).

state. These numbers are based on the definition of a sharp peak as a peak with an intensity 5 times higher than the nonsharp peaks and, for M4-N, with ^1H-^{15}N NOE values of less than around 0.2. Because M22-NL is identical to M22-N except for the *C*-terminal extension, the 10 extra flexible residues in M22-N compared to those in M22-NL should be located in the *C*-terminus of M22-N. It thus appears as if the coiled coil is less stable in M22-N than in M22-NL. The flexibility of the 10 most *C*-terminal residues in M22-N may be due to the unfavorable positioning of the disulfide bond in this peptide.

Chemical Shift Indexing of M4-N. The ^{13}C chemical shift of the α- and carbonyl carbon (C′) depends on protein conformation (*38*−*40*). Therefore, we calculated the chemical shift displacement from random coil values (*39*, *41*) for the assigned residues in M4-N (Figure 4). The chemical shift displacements are consistent with α-helical conformation for at least residues 19−37. The lack of assignments prohibits the analysis of residues 13−18, but the $^{13}C^\alpha$ shifts for residues 1−12 and 40−46 are close to the random coil values, consistent with the relaxation measurements (see below), indicating that these parts of the molecule are disordered. It has previously been observed that a heptadic repeat pattern can be found in the chemical displacements of H^N (upfield shift of a and d positions and downfield shifts of c positions compared to nearby residues) and C′ (upfield shift of c and downfield shift of a and e positions compared to nearby residues) for coiled coils (*40*, *42*, *43*). A clear repeat pattern can be found in the C′ displacements with downfield shifts for a and d positions as well as upfield shifts for c positions in the region Y18 to Y35. This is consistent with the formation of coiled coil in that region (Figure 4). This heptadic repeat pattern is also predicted by the COILS (*31*) algorithm. For the H^N displacements, the repeat pattern is not as clear although the general trend is as expected.

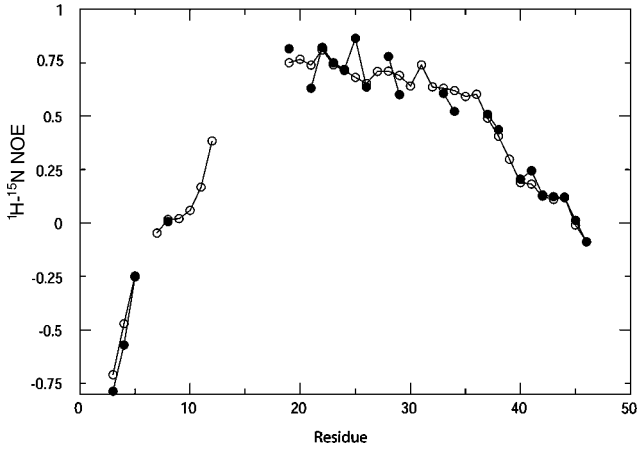

FIGURE 5: ^1H-^{15}N NOE values for M4-N at 0.1 mM (●) and 1 mM (○) concentration.

Because of the smaller chemical shift range and concentration dependence of the chemical shifts, this is not unexpected.

Dynamical Properties of M4-N. ^1H-^{15}N NOE values report on the structural organization on a per-residue basis and were determined for M4-N at 0.1 and 1 mM (Figure 5) concentration. The NOE values were found to be independent of M4-N concentration and show that M4-N has flexible *N*- and *C*-terminal regions. Roughly 11 *N*-terminal and 6 *C*-terminal residues are flexible in M4-N. The *C*-terminal residues have larger NOE values consistent with the disulfide linkage that reduces their conformational freedom compared to that in free termini. The flexibility of the *C*-terminus is unexpected because the preferred conformation based on sequence is a coiled coil. However, it could be a consequence of an unfavorable placement of the disulfide linkage. The NOE values for the center residues are as large as those found for other coiled-coil proteins of similar size (*42*) and show that M4-N has a folded central region.

The NMR relaxation rates of a molecule are sensitive probes of its hydrodynamic properties. The R_2 values are especially sensitive to the global rotational correlation time of a protein, and it can be shown that for an isotropically tumbling protein the R_2/R_1 ratio is a direct function of the correlation time. For a nonisotropically tumbling protein (such as M4-N), the situation is more complicated because the rotation of the molecule cannot be characterized by a single correlation time. For M4-N, we observed high R_2/R_1 ratios (close to 20) for the central residues 19−36 and significantly lower values (around 2−5) for terminal residues (3−10 and 38−46) (Figure 6A). These results are in agreement with flexible ends and a folded coiled coil in the central region of M4-N. The relaxation measurements were conducted at low concentration to avoid aggregation.

Residual Dipolar Couplings. An alignment medium was used to partially order the protein in the magnetic field with the long axis in the direction of the static field. In such a medium, the residual dipolar couplings (RDCs) can be measured. Because all ^1H-^{15}N bond vectors are pointing in the same direction in a coiled coil, it is expected that a measurement of ^1H-^{15}N RDCs would give values with equal signs and similar magnitudes for all residues in the coiled-coil conformation. Only 23 dipolar couplings were measured for M4-N because of spectral overlap (Figure 7A). These measured RDCs showed a negative sign for the center

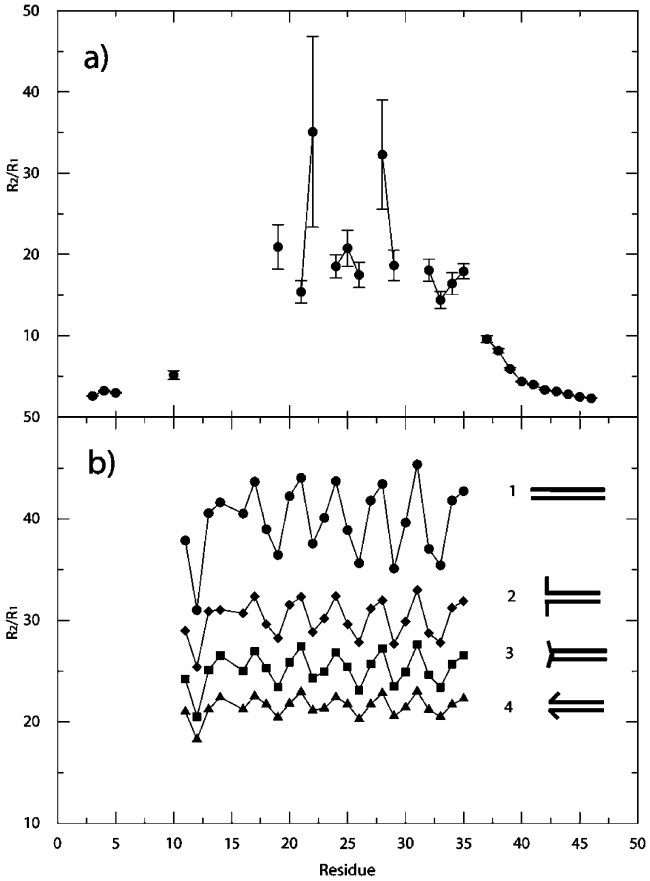

FIGURE 6: Ratio of longitudinal (R_2) and transverse (R_1) relaxation rates of 0.1 mM M4-N. (A) Experimental and (B) calculated values from hydrodynamic modeling with HydroNMR 22 using the model of M4-N with four different conformations of the flexible 10 *N*-terminal residues, as indicated. The numbers refer to the description in the text.

residues, as expected for a coiled-coil region, whereas low or zero values were observed for the residues at the ends as expected for flexible residues.

Modeling of M4-N. On the basis of the results from the NMR study, the 3D structure of M4-N was modeled. The full-length M4 protein has high coiled-coil propensity throughout the sequence, including the HVR, as predicted by the COILS (*31*) algorithm. The predicted heptadic repeat pattern was used in a sequence alignment with the SIR4 protein from *S. cerevisiae*, the 3D structure (*32*) of which served as a template for homology modeling. This protein was chosen as the template because it is one of the very few parallel dimeric coiled-coiled structures with significant length found in the pdb database. The resulting model should accurately represent the backbone fold of the coiled coil, but the exact location of the side-chains will be less certain. M4-N was modeled as a parallel coiled coil, encompassing the first 38 residues and a *C*-terminal loop including residues 39−46 connected via the disulfide bond (Figure 8). In this model, the conformation of flexible residues 1−12 and 39−46 is arbitrary, as are the conformations of side chains that point toward the solvent.

We performed hydrodynamic modeling using our M4-N model to provide predicted R_2/R_1 values (Figure 6B) that are compared to the experimental values (Figure 6A). The predicted R_2/R_1 ratios depend on whether the *N*-terminal flexible residues are included in the hydrodynamic simulation, and a good agreement between simulation and experiment is obtained if the first six residues are excluded. To investigate the dependence of the result of this simulation on the conformation of the flexible *N*-terminal residues, four different conformations of the first 10 residues in the peptide were simulated (Figure 6B): (1) a fully extended coiled coil, (2) each segment pointing perpendicular to the principal axis of the coil extending out from the center of the coil, (3) each segment pointing perpendicular to the principal axis of the coiled coil extending to the center of the coil, and (4) each segment bending forward along the principal axis of the coiled-coil. The average R_2/R_1 values for these conformers are 40, 30, 25, and 20, respectively. The actual value would be found as an ensemble average of all conformations of the flexible ends but will fall in the range of 20−40 so that the experimental result of $R_2/R_1 = 20$ for the central residues can be reproduced in simulations using our model. It is clear that the measured R_2/R_1 ratios are consistent with an extended shape of a large central portion and are also found to be similar to those found experimentally for other coiled coils of similar size (*42*).

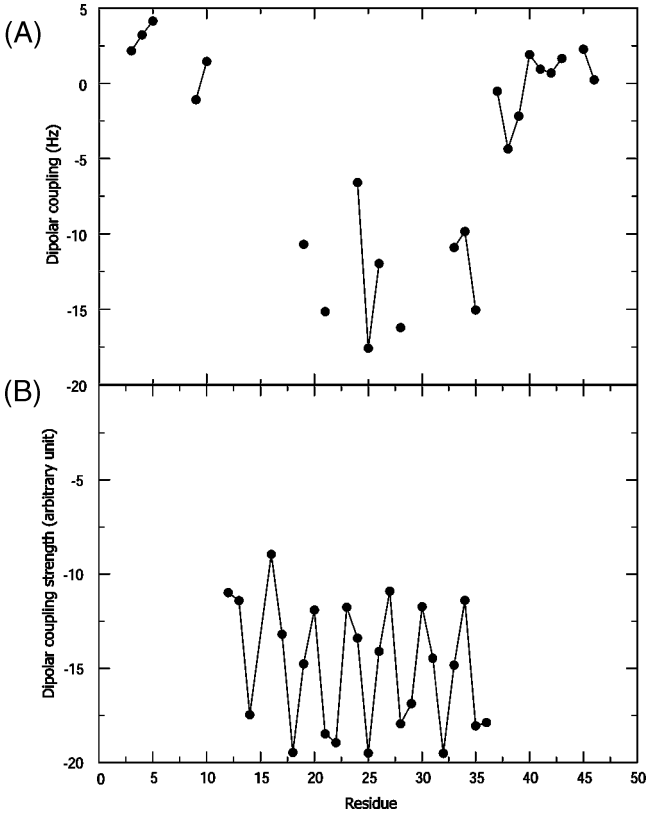

FIGURE 7: Dipolar couplings. (A) Measured values for 0.1 mM M4-N in a 3% C12E5/*n*-hexanol medium. (B) Calculated values using the model of M4-N and the computer program Pales (*30*).

Our structural model of M4-N was also used in a theoretical calculation of RDCs. These calculated RDCs (Figure 7B) are in qualitative agreement with the experiment data (Figure 7A). We did not try to predict the absolute values of the dipolar couplings because of the inherent uncertainties. However, the relative order of the values of the dipolar couplings in the center of the molecule is predicted correctly by the model, further strengthening the coiled-coil hypotheses.

Peptide Binding to C4BPα-CCP1-2. A major binding site for M proteins in C4BP is located in the first two CCP

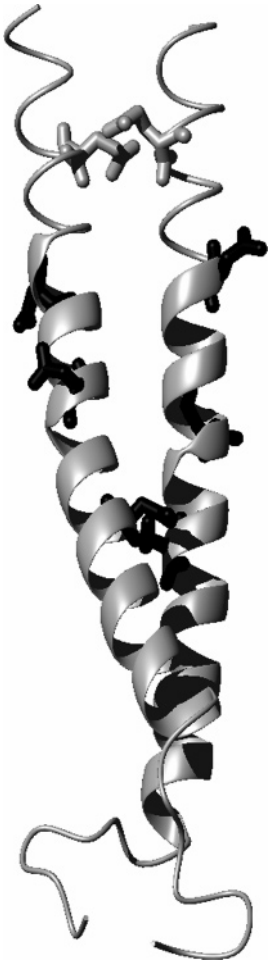

FIGURE 8: Model of M4-N as a dimeric coiled coil. Residues N13, N19, and N25 are shown in black and Q7 in gray.

modules of the α-chain that are contained in the fragment CCP1-2 (*5*, *7*). The binding of M4-N, M22-N, and M22-NL to C4BPα-CCP1-2 was studied by the titration of ^{15}N-labeled peptides to C4BPα-CCP1-2. The final solution that was used to study the bound form of the M-peptide contained a 5-fold excess of C4BPα-CCP1-2 over the peptide (Figure 3). This large excess was chosen to guarantee that the observed HSQC spectra represented the peptides in complex with C4BPα-CCP1-2, although the aggregation of C4BPα-CCP1-2 can somewhat change the ratio present in the solution. Comparisons of the ^{1}H-^{15}N HSQC spectra for bound and unbound peptides show that all M protein constructs bind C4BPα-CCP1-2. For all peptides, there is a loss of a number of resonances in the bound state, and the spectral quality is poor. The M4-N complex with C4BPα-CCP1-2 was studied in detail. Here, only 17 out of 43 (46 minus the *N*-terminal residue and 2 prolines) resonances were seen. Four of them are found in the same position as in the spectrum of free M4-N, and these could be identified as residues E2-K4 and C46. It is clear that the resonances that are visible in the complex of M4-N and C4BPα-CCP1-2 represent flexible residues. This result indicates that 28 residues are within the binding region (46 residues minus 17 residues and *N*-terminal residue), although it does not mean that all residues are directly involved in complex formation. (If M4-N binds as a coiled coil, then approximately half of the residues are likely to directly interact with C4BPα-CCP1-2.) The fact that most of the flexible residues display chemical shift changes compared to the free peptide is not unexpected in a linear fold such as the coiled coil where the chemical shift will be affected by the conformational changes of nearby residues in the peptide chain and the proximity to C4BPα-CCP1-2. It can be deduced from the titration experiments that M4-N binds with slow exchange on the NMR time scale as seen from the gradual appearance of the free signal (data not shown). For the complex of M22-N or M22-NL with C4BPα-CCP1-2, 25 and 16 peaks are seen in the respective spectra. Using the same argument as that for M4-N, these numbers indicate that 27 residues of M22-N are involved in complex formation. We expected more peaks to remain in the spectrum of C4BPα-CCP1-2 in complex with M22-NL than with M22-N, but it is probable that the rotational properties of the M22-NL complex led to severe broadening of resonances. This can be seen as larger line widths of the backbone and side-chains resonances in the HSQC spectra of the complex of M22-NL compared to those of the free peptide and other complexes (Figure 3).

Assignment of Asn and Gln Side-Chain Resonances in the M4-N C4BPα-CCP1-2 Complex. M4-N contains one Gln and three Asn residues, and the amide groups of all four side chains are observed in the HSQC spectrum of free M4-N. However, in the complex of M4-N with C4BPα-CCP1-2, only one of these side-chain amides is visible. The assignment of this residue may provide additional information on the binding region that should contain the three side chains with the disappearing resonances. The titration of ^{15}N-^{13}C labeled M4-N to C4BPα-CCP1-2 was therefore monitored using a modified CBCA(CO)NH pulse sequence optimized for detecting side-chain correlations. The observed ^{13}C shifts at 29.5 and 34 ppm are consistent with Gln but not with Asn. (Gln has on average 29.2 ppm for C^{β} and 33.7 ppm for C^{γ}, whereas Asn has 53.5 ppm for C^{α} and 38.6 ppm for C^{β}; Biomagnetic Resonance Data Bank, http://www.bmrb.wisc.edu.) The single side-chain resonance of the HSQC spectra could therefore be assigned to Q7. On the basis of this assignment, we conclude that N13, N19, and N25 side-chain resonances are lost upon complex formation and that these residues are part of the binding region. The loss of the signal is due to either the immobilization of these residues in the complex or the conformational exchange.

DISCUSSION

The hypervariable C4BP-binding regions of M proteins from different *S. pyogenes* strains have only few conserved residues (*6*). Remarkably, the studies of isolated HVRs from three different strains show that they have no immunological crossreactivity despite the high affinity for C4BP (*6*). If we assume that HVRs adopt a similar structural fold, which is the most reasonable assumption, this represents a paradox. This apparent paradox may be resolved if antibodies and C4BP recognize different surfaces of the HVR and/or utilize different binding mechanisms. One explanation for this situation could be a folding upon binding mechanism in which the HVRs are unstructured until they bind to C4BP or to an antibody. Another explanation could be that the HVRs adopt the same fold when bound to C4BP and an antibody, whereas the latter proteins recognize different components of the HVRs, such as the general backbone fold or side chains. In a third scenario, the HVRs could be folded by themselves, but the binding to C4BP or an antibody could

lead to a conformational rearrangement of the HVRs inducing a common structure in the HVRs, whereas the unbound HVRs have different structures. The data reported here allow us to distinguish between these scenarios.

Taken together, our data indicate that the free HVRs are folded as coiled coils with flexible termini. Indeed, the CD spectra show that a significant fraction of each peptide is in helical conformation, indicating that the peptides adopt coiled-coil structures, and the CD and NMR spectra show similar features for all three peptides M4-N, M22-N, and M22-NL, indicating a similar structure. Detailed studies were focused on the M4-N peptide. The limited chemical-shift dispersion of ^{1}H-^{15}N HSQC spectra for M4-N is consistent with an α-helical conformation. Chemical-shift displacements in $^{13}C^{\alpha}$ and $^{13}C'$ carbonyl clearly indicate that residues 1−12 and 40−46 are disordered and that residues 19−39 are in α-helical conformation. In addition, the presence of a number of sharp and more intense peaks in the ^{1}H-^{15}N HSQC spectra and resonance assignments allow us to conclude that residues 1−12 and 40−46 are flexible, whereas the central 27 residues of M4-N form the coiled-coil region.

On the basis of the spectroscopic data, the coiled-coil propensities and the heptadic repeat pattern of the amino acid sequence, a homology model of M4-N was constructed. Using this model, the physical parameters of M4-N were predicted and compared with experimental values. Both the R_2/R_1 ratios and RDC values, which report on structural confinement of different regions of the peptide, are consistent with the model. The experimental values are also similar to values determined for other coiled-coil proteins of similar size. Also, the correct pattern of minima and maxima in the RDC values is predicted from the model. Chemical-shift displacements show that the center of the molecule has a α-helical conformation. Furthermore, the chemical-shift displacements of the ^{13}C carbonyls display a heptadic repeat pattern from Y18 to Y35, which is consistent with the heptadic repeat pattern predicted from COILS. This presents a clear indication that M4-N adopts a coiled-coil structure in this region. Although our M4-N model agrees with all experimental results, it may be wise to also consider alternative models with helical structure such as a helix−loop−helix motif (*6*). However, we found no experimental evidence for a loop region in the middle of the peptide with different R_2/R_1 ratios and chemical-shift displacements. Finally, the HVRs of M4-N, M22-N, and M22-NL, all have high coiled-coil propensities. In conclusion, we propose that M4-N and most likely M22-N/M22-NL in solution adopts a coiled-coil structure with flexible ends.

Our NMR data also allow us to discuss the conformation of a peptide bound to C4BPα-CCP1-2. The backbone resonances of all residues that are directly involved in binding disappear in the HSQC spectrum of the complex. This allows us to map the binding surface and conclude that as many as roughly 28 residues are found in the binding region. Only resonances of residues that are flexible in the complex are observed, and, therefore, we cannot directly study the conformation of the peptide bound in the complex. Using side-chain amide assignments, we can also conclude that N13, N19, and N25 are part of the binding region, whereas Q7 is not.

From the arguments presented above, we can rule out a folding upon binding mechanism because the C4BP binding region of M4-N is found within the 27 residues that form the folded coil-coil region in the free state, whereas the rest of the residues are flexible both in free M4-N and in complex with C4BP. Moreover, our data indicate that the unbound HVRs have similar structures. Thus, we tentatively conclude that different C4BP-binding HVRs adopt the same fold but nevertheless are antigenically unrelated. Considering the high sequence diversity of HVRs from different strains of *S. pyogenes*, a reasonable scenario is that C4BP recognizes the backbone fold of the HVR, whereas the interactions of antibodies are more side-chain oriented.

Altogether, our data show that the C4BP binding region in the M4-N peptide is elongated and comprises as many as four heptadic repeats. This finding suggests that the binding region may be as long as 35 Å and, therefore, capable of simultaneously contacting each of the two *N*-terminal CCP modules of the C4BP α-chain. High-resolution structures (*44*−*46*) show that CCP modules are prolate ellipsoids with dimensions of roughly 40 × 15 × 15 Å^3, with consecutive modules aligned along the long axis but with a slightly bent structure with intermodule angles of 20−40°. Protein engineering data show that both CCP1 and CCP2 are needed for the binding of M proteins (*7*) (A. M. Blom, unpublished results), and a recent NMR study of ^{15}N-labeled C4BPα-CCP1-2 in complex with unlabeled M4-N revealed chemical-shift changes in both CCP modules (*47*).

In conclusion, the *N*-terminal hypervariable region of M4 has a folded nucleus of ∼27 residues that adopts a coiled-coil structure in solution. The C4BP binding region of M4-N is found within the same 27 residues, whereas the remaining residues are flexible both in free M4-N and in complex with C4BP. Our data further suggest that despite extensive differences in the primary sequence between M4-N and M22-N, these two C4BP binding domains seem to adopt similar folds, both in solution and in complex with C4BPα-CCP1-2.

ACKNOWLEDGMENT

The monoclonal antibody against C4BP was a kind gift by Professor Björn Dahlbäck (Lund University). We acknowledge the Swedish NMR Centre for the use of the spectrometers.

REFERENCES

1. Kehoe, M. A. (1994) Cell-wall-associated proteins in Gram-positive bacteria, *New Compr. Biochem. 27*, 217−261.
2. Facklam, R. F., Martin, D. R., Lovgren, M., Johnson, D. R., Efstratiou, A., Thompson, T. A., Gowan, S., Kriz, P., Tyrrell, G. J., Kaplan, E., and Beall, B. (2002) Extension of the Lancefield classification for group A streptococci by addition of 22 new M protein gene sequence types from clinical isolates: *emm*103 to *emm*124, *Clin. Infect. Dis. 34*, 28−38.
3. Thern, A., Stenberg, L., Dahlbäck, B., and Lindahl, G. (1995) Ig-binding surface proteins of *Streptococcus* pyogenes also bind human C4b-binding protein (C4BP), a regulatory component of the complement system, *J. Immunol. 154*, 375−386.
4. Johnsson, E., Thern, A., Dahlbäck, B., Heden, L. O., Wikström, M., and Lindahl, G. (1996) A highly variable region in members of the streptococcal M protein family binds the human complement regulator C4BP, *J. Immunol. 157*, 3021−3029.
5. Blom, A. M., Berggård, K., Webb, J. H., Lindahl, G., Villoutreix, B. O., and Dahlbäck, B. (2000) Human C4b-binding protein has overlapping, but not identical, binding sites for C4b and streptococcal M proteins, *J. Immunol. 164*, 5328−5336.
6. Morfeldt, E., Berggård, K., Persson, J., Drakenberg, T., Johnsson, E., Lindahl, E., Linse, S., and Lindahl, G. (2001) Isolated

hypervariable regions derived from streptococcal M proteins specifically bind human C4b-binding protein: implications for antigenic variation, *J. Immunol. 167*, 3870−3877.
7. Accardo, P., Sanchez-Corral, P., Criado, O., Garcia, E., and Rodriguez de Cordoba, S. (1996) Binding of human complement component C4b-binding protein (C4BP) to *Streptococcus pyogenes* involves the C4b-binding site, *J. Immunol. 157*, 4935−4939.
8. Fujita, T., Gigli, I., and Nussenzweig, V. (1978) Human C4-binding protein. II. Role in proteolysis of C4b by C3b-inactivator, *J. Exp. Med. 148*, 1044−1051.
9. Gigli, I., Fujita, T., and Nussenzweig, V. (1979) Modulation of the classical pathway C3 convertase by plasma proteins C4 binding protein and C3b inactivator, *Proc. Natl. Acad. Sci. U.S.A. 76*, 6596−6600.
10. Dahlbäck, B. (1991) Protein S and C4b-binding protein: components involved in the regulation of the protein C anticoagulant system, *Thromb. Haemostasis 66*, 49−61.
11. Carlsson, F., Berggård, K., Stålhammar-Carlemalm, M., and Lindahl, G. (2003) Evasion of phagocytosis through cooperation between two ligand-binding regions in *Streptococcus pyogenes* M protein, *J. Exp.* Med. *198*, 1057−1068.
12. Phillips, G. N., Jr., Flicker, P. F., Cohen, C., Manjula, B. N., and Fischetti, V. A. (1981) Streptococcal M protein: alpha-helical coiled-coil structure and arrangement on the cell surface, *Proc. Natl. Acad. Sci. U.S.*A. *78*, 4689−4693.
13. Fischetti, V. A. (1989) Streptococcal M protein: molecular design and biological behavior. *Clin. Microbiol. Rev. 2*, 285−314.
14. Cedervall, T., Johansson, M. U., and Åkerström, B. (1997) Coiled-coil structure of group A streptococcal M proteins. Different temperature stability of class A and C proteins by hydrophobic-nonhydrophobic amino acid substitutions at heptad positions a and d, *Biochemistry 36*, 4987−4994.
15. Nilson, B. H., Frick, I. M., Åkesson, P., Forsen, S., Björck, L., Åkerström, B., and Wikström, M. (1995) Structure and stability of protein H and the M1 protein from *Streptococcus pyogenes*. Implications for other surface proteins of gram-positive bacteria, *Biochemistry 34*, 13688−13698.
16. McNeil, S. A., Halperin, S. A., Langley, J. M., Smith, B., Warren, A., Sharratt, G. P., Baxendale, D. M., Reddish, M. A., Hu, M. C., Stroop, S. D., Linden, J., Fries, L. F., Vink, P. E., and Dale, J. B. (2005) Safety and immunogenicity of 26-valent group A streptococcus vaccine in healthy adult volunteers, *Clin. Infect. Dis. 41*, 1114−1122.
17. Frithz, E., Hedén, L. O., and Lindahl, G. (1989) Extensive sequence homology between IgA receptor and M proteins in *Streptococcus pyogenes*, *Mol. Microbiol. 3*, 1111−1119.
18. Stenberg, L., O'Toole, P. W., Mestecky, J., and Lindahl, G. (1994) Molecular characterization of protein Sir, a streptococcal cell surface protein that binds both immunoglobulin A and immunoglobulin G, *J. Biol. Chem. 269*, 13458−13464.
19. Heiring, C., and Muller, Y. A. (2001) Folding screening assayed by proteolysis: application to various cystine deletion mutants of vascular endothelial growth factor, *Protein Eng. 14*, 183−188.
20. Härdig, Y., Hillarp, A., and Dahlbäck, B. (1997) The amino-terminal module of the C4b-binding protein alpha-chain is crucial for C4b binding and factor I-cofactor function, *Biochem. J. 323*, 469−475.
21. Delaglio, F., Grzesiek, S., Vuister, G. W., Zhu, G., Pfeifer, J., and Bax, A. (1995) NMRPipe: a multidimensional spectral processing system based on UNIX pipes, *J. Biomol. NMR 6*, 277−293.
22. Kay, L. E., Keifer, P., and Saarinen, T. (1992) Pure absorption gradient enhanced heteronuclear single quantum correlation spectroscopy with improved sensitivity, *J. Am. Chem. Soc. 114*, 10663−10665.
23. Kay, L. E., Ikura, M., Tschudin, R., and Bax, A. (1990) 3-dimensional triple-resonance NMR-spectroscopy of isotopically inriched proteins, *J. Magn. Reson. 89*, 496−514.
24. Grzesiek, S., and Bax, A. (1992) Correlating backbone amide and side-chain resonances in larger proteins by multiple relayed triple resonance NMR, *J. Am. Chem. Soc. 114*, 6291−6293.
25. Lohr, F., and Rüterjans, H. (1995) A new triple-resonace experiment for the sequential assignment of backbone resonances in proteins, *J. Biomol. NMR 6*, 189−197.
26. Farrow, N. A., Muhandiram, R., Singer, A. U., Pascal, S. M., Kay, C. M., Gish, G., Shoelson, S. E., Pawson, T., Forman-Kay, J. D., and Kay, L. E. (1994) Backbone dynamics of a free and phosphopeptide-complexed Src homology 2 domain studied by ^{15}N NMR relaxation, *Biochemistry 33*, 5984−6003.
27. Garcia de la Torre, J., Huertas, M. L., and Carrasco, B. (2000) HYDRONMR: prediction of NMR relaxation of globular proteins from atomic-level structures and hydrodynamic calculations, *J. Magn. Reson. 147*, 138−146.
28. Ruckert, M., and Otting, G. (2000) Alignment of biological macromolecules in novel nonionic liquid crystalline media for NMR experiments, *J. Am. Chem. Soc. 122*, 7793−7797.
29. Ottiger, M., Delaglio, F., and Bax, A. (1998) Measurement of J and dipolar couplings from simplified two-dimensional NMR spectra, *J. Magn. Reson. 131*, 373−378.
30. Zweckstetter, M., and Bax, A. (2000) Prediction of sterically induced alignment in a dilute liquid crystalline phase: Aid to protein structure determination by NMR, *J. Am. Chem. Soc. 122*, 3791−3792.
31. Lupas, A., Vandyke, M., and Stock, J. (1991) Predicting coiled coils from protein sequences, *Science 252*, 1162−1164.
32. Murphy, G. A., Spedale, E. J., Powell, S. T., Pillus, L., Schultz, S. C., and Chen, L. (2003) The Sir4 C-terminal coiled coil is required for telomeric and mating type silencing in *Saccharomyces cerevisiae*, *J. Mol. Biol. 334*, 769−780.
33. Sali, A., and Blundell, T. L. (1993) Comparative protein modelling by satisfaction of spatial restraints, *J. Mol. Biol. 234*, 779−815.
34. Sandin, C., Linse, S., Areschoug, T., Woof, J. M., Reinholdt, J., and Lindahl, G. (2002) Isolation and detection of human IgA using a streptococcal IgA-binding peptide, *J. Immunol. 169*, 1357−1364.
35. Lau, S. Y., Taneja, A. K., and Hodges, R. S. (1984) Synthesis of a model protein of defined secondary and quaternary structure. Effect of chain length on the stabilization and formation of two-stranded alpha-helical coiled-coils, *J. Biol. Chem. 259*, 13253−13261.
36. Engel, M., Williams, R. W., and Erickson, B. W. (1991) Designed coiled-coil proteins: Synthesis and spectroscopy of two 78-residue alpha-helical dimers, *Biochemistry 30*, 3161−9.
37. Cedervall, T. (1999) Temperature-dependent structure and function of group A streptococcal M proteins, Ph.D. Thesis, Lund University, Lund, Sweden.
38. Wishart, D. S., Sykes, B. D., and Richards, F. M. (1992) The chemical shift index: A fast and simple method for the assignment of protein secondary structure through NMR spectroscopy, *Biochemistry 31*, 1647−1651.
39. Wishart, D. S., and Sykes, B. D. (1994) The ^{13}C chemical-shift index: a simple method for the identification of protein secondary structure using ^{13}C chemical-shift data, *J. Biomol. NMR 4*, 171−180.
40. Goodman, E. M., and Kim, P. S. (1991) Periodicity of amide proton exchange rates in a coiled-coil leucine zipper peptide, *Biochemistry 30*, 11615−11620.
41. Wüthrich, K. (1986) *NMR of Proteins and Nucleic Acids*, John Wiley and Sons, New York.
42. Greenfield, N. J., Swapna, G. V., Huang, Y., Palm, T., Graboski, S., Montelione, G. T., and Hitchcock-DeGregori, S. E. (2003) The structure of the carboxyl terminus of striated alpha-tropomyosin in solution reveals an unusual parallel arrangement of interacting alpha-helices, *Biochemistry 42*, 614−619.
43. Kuntz, I. D., Kosen, P. A., and Craig, E. C. (1991) Amide chemical-shifts in many helices in peptides and proteins are periodic, *J. Am. Chem. Soc. 113*, 1406−1408.
44. Barlow, P. N., Norman, D. G., Steinkasserer, A., Horne, T. J., Pearce, J., Driscoll, P. C., Sim, R. B., and Campbell, I. D. (1992) Solution structure of the fifth repeat of factor H: A second example of the complement control protein module, *Biochemistry 31*, 3626−3634.
45. Henderson, C. E., Bromek, K., Mullin, N. P., Smith, B. O., Uhrin, D., and Barlow, P. N. (2001) Solution structure and dynamics of the central CCP module pair of a poxvirus complement control protein, *J. Mol.* Biol. *307*, 323−339.
46. Blein, S., Ginham, R., Uhrin, D., Smith, B. O., Soares, D. C., Veltel, S., McIlhinney, R. A., White, J. H., and Barlow, P. N. (2004) Structural analysis of the complement control protein (CCP) modules of GABA(B) receptor 1a: only one of the two CCP modules is compactly folded, *J. Biol. Chem. 279*, 48292−48306.
47. Jenkins, H. T., Mark, L., Ball, G., Persson, J., Lindahl, G., Uhrin, D., Blom, A. M., Barlow, P. N. (2006) Human C4b-binding protein − structural basis for interaction with Streptococcal M protein, a major bacterial virulence factor, *J. Biol. Chem. 281*, 690−697.

BI052455C